International Journal of Computational and Experimental Science and Engineering (IJCESEN)

Vol. 11-No.4 (2025) pp. 10262-10282
https://www.ijcesen.com

ISSN: 2149-9144

Copyright © IJCESEN

Research Article

Experimental Investigation and Predictive Modelling of Sustainable Concrete Incorporating Industrial By-Products

Chethan Kumar N T[1*], K E Prakash[2], Supriya M J[3], Brunda B N[4]

[*1,2]Department of Civil Engineering, [*1]Research Scholar, Shree Devi Institute of Technology, Mangalore-574 142, Visvesvaraya Technological University, Belagavi-590018, Karnataka, India.
* **Corresponding Author Email:** chethancv.mce@gmail.com- **ORCID:** 0000-0001-7193-4001

[2]Professor, Shree Devi Institute of Technology, Mangalore-574 142, Visvesvaraya Technological University, Belagavi-590018, Karnataka, India.
Email: prakashke@yahoo.co.in-**ORCID:** 0000-0003-3901-4015

[3]Associate Professor, Department of Civil Engineering, Malnad College of Engineering, Hassan-573201, Karnataka, India.
Email: smj@mcehassan.ac.in-**ORCID:** 0000-0003-3901-4015

[4]Assistant Professor, Department of Civil Engineering, Malnad College of Engineering, Hassan-573201, Karnataka, India.
Email: brb@mcehassan.ac.in-**ORCID:** 0000-0003-3901-4015

Article Info:

DOI: 10.22399/ijcesen.4824
Received: 10 October 2025
Revised: 20 December 2025
Accepted: 25 December 2025

Keywords

GGBS
Fly ash
Marble dust
Laterite
Machine learning
Mechanical properties

Abstract:

The increasing demand for concrete structures has led to the overexploitation of natural resources such as river sand and stone aggregates. This study explores sustainable alternatives by incorporating industrial by-products like fly ash and marble dust, along with laterite and demolition debris, as partial replacements in M30-grade concrete. Ground Granulated Blast Furnace Slag (GGBS) was used as an ad IJ Iditive in all mix proportions. Concrete mixes were prepared and tested for compressive, flexural, split tensile strengths water absorption, sorptivity and RCPT. The 10% fly ash mix achieved a compressive strength of 45.09 MPa after 28 days, closely matching the control mix (46.74 MPa). However, 20% and 30% marble dust replacements resulted in reduced strengths of 28.65 MPa and 29.84 MPa, respectively. The 10% laterite mix exhibited the highest compressive strength (48.46 MPa), surpassing conventional concrete. Flexural and split tensile strength results followed similar trends, with fly ash and laterite improving mechanical properties, while excessive marble dust reduced tensile performance. To enhance predictive accuracy and optimize mix design, machine learning models were employed. The Random Forest Regression model demonstrated the highest prediction accuracy (R^2= 0.92), outperforming traditional regression models. The integration of machine learning enabled efficient analysis, identifying key parameters affecting concrete performance. This study highlights the potential of sustainable materials in concrete production and underscores the role of data-driven approaches in optimizing mechanical properties for eco-friendly construction.

1. Introduction

Concrete is the most widely used construction material worldwide, owing to its excellent mechanical properties, durability, and versatility. It is estimated that over 30 billion tons of concrete are produced annually, making it the second most consumed material after water (Hussain et al. 2023; Liu et al. 2023a; Ujwal et al. 2025). However, the extensive use of conventional concrete raises significant environmental concerns, primarily due to the high carbon footprint associated with cement production. Cement manufacturing alone accounts for approximately 8% of global CO_2 emissions

(Ahmad et al. 2022; Aslani et al. 2023; Joseph et al. 2023). Consequently, researchers have explored alternative supplementary materials to partially replace cement and aggregates, reducing the environmental impact while maintaining or improving concrete performance. Among the most studied materials are Ground Granulated Blast Furnace Slag (GGBS), Fly Ash (FA), and Demolition Waste (DW), all of which contribute to sustainable construction practices (Ahmad et al. 2022; Aslani et al. 2023; Joseph et al. 2023; Mali et al. 2022; Mohamed et al. 2023; Singh et al. 2019). Cement is a key binding material in concrete, with Portland cement (OPC) being the most commonly used type. The global cement industry produces approximately 4.1 billion metric tons of cement per year, with China, India, and the European Union as leading producers. The production of 1 ton of OPC emits nearly 0.9 tons of CO_2, largely due to the calcination of limestone and energy-intensive clinker production (Chun et al. 2023; Singh et al. 2023). With rising urbanization and infrastructure demands, reducing cement usage in concrete has become a crucial research focus. GGBS is an industrial byproduct obtained from the steel manufacturing process (Guo et al. 2018; Ulubeyli and Artir 2015). It has been widely used as a partial cement replacement due to its pozzolanic properties, which enhance the strength and durability of concrete. Studies have shown that replacing 30-50% of cement with GGBS can significantly reduce heat of hydration, improve sulphate resistance, and lower CO_2 emissions by nearly 40% (Hussain et al. 2023; Luo et al. 2023).

The global marble industry generates millions of tons of waste annually, with marble dust constituting a significant portion. Research indicates that 10-30% replacement of cement with marble dust improves concrete's compressive strength, reduces permeability, and enhances its aesthetic appeal. The fine particles of marble dust fill voids in the cement matrix, leading to denser and more durable concrete. However, excessive replacement beyond 30% may negatively impact strength due to reduced cementitious material (Atta and Bakhoum 2024; Olutoge and Modupeola 2014). Fly ash, a by-product of coal combustion in thermal power plants, is a well-established pozzolanic material used in concrete production. Over 750 million tons of fly ash are generated globally every year, yet only 60 - 65% is utilized in construction. Fly ash improves workability, reduces heat of hydration, and enhances long-term strength development. Research suggests that concrete with 20-40% fly ash replacement can achieve comparable or even superior performance to traditional OPC concrete, while simultaneously reducing CO_2 emissions by 25-35% (Cheng et al. 2023; Liu et al. 2023b).Laterite is a soil type rich in iron and aluminium, commonly found in tropical regions. Its use in concrete has gained interest due to its availability and potential to replace natural fine aggregates, which are becoming increasingly scarce. Studies have shown that 10-30% replacement of sand with laterite can result in comparable compressive strength while improving thermal insulation properties. However, laterite's high-water absorption may necessitate the use of water-reducing admixtures to maintain workability (Aliabdo et al. 2014; Ettu et al. 2013). The construction and demolition industry generates approximately 1.3 billion tons of waste annually, with concrete and masonry debris constituting nearly 40% of this total. Recycling demolition waste as coarse or fine aggregate in new concrete production has emerged as a sustainable solution to reduce landfill disposal and conserve natural resources (Handayani et al. 2023; Ujwal and Shiva Kumar 2024; Zhao et al. 2023). Research has demonstrated that 20-50% replacement of natural aggregates with recycled demolition waste can maintain acceptable strength and durability parameters, provided that contaminants such as plaster and wood are minimized. Additionally, the use of recycled aggregates significantly reduces embodied energy in concrete, contributing to overall sustainability goals. Several studies have compared the performance of concrete incorporating these alternative materials. A meta-analysis by (Ahmad et al. 2022; Kumar et al. 2025) found that concrete mixes with 30% GGBS, 20% fly ash, and 10% marble dust exhibited 15-20% higher durability compared to conventional OPC concrete.

(El Khessaimi et al. 2023; Ujwal et al. 2025) conducted an experimental study on the mechanical properties of concrete with 40% GGBS replacement. The results indicated a 15% increase in compressive strength at 56 days compared to conventional concrete. Additionally, durability tests showed enhanced resistance to chloride and sulphate attacks, making GGBS an effective alternative material for infrastructure exposed to harsh environments (Wang et al. 2024) investigated the impact of 10-30% marble dust replacement on concrete strength and durability. The study concluded that a 20% replacement yielded the highest compressive strength, while beyond this threshold, strength decreased due to excessive filler effect. Marble dust also contributed to reduced permeability, enhancing the sustainability of the mix. Malhotra & Mehta (2019) analysed the long-term performance of fly ash-based concrete. Their research demonstrated that 25% fly ash substitution resulted in 30% lower CO_2 emissions and increased workability. However, early-age strength gain was slower, requiring a longer curing period to achieve optimal performance (Mali et al. 2022) examined the feasibility of

replacing sand with laterite in concrete mixes. However, higher replacements required admixtures to balance workability and water absorption issues (Zia et al. 2023) studied the performance of recycled demolition waste as coarse aggregate. The research found that 30% replacement of natural aggregates with demolition waste maintained structural integrity while reducing embodied carbon by 20%. The study emphasized proper sorting and treatment of recycled materials to ensure uniform quality.

Despite extensive research on sustainable concrete, there remains a gap in understanding the combined effects of fly ash, marble dust, laterite, and demolition debris as alternative materials in concrete. While individual studies have explored these materials separately, limited research has examined their integrated impact on the mechanical properties of concrete structures. Furthermore, the use of machine learning models for predicting the compressive strength of such sustainable concrete mixes is still in its early stages. Traditional experimental approaches, though effective, can be time-consuming and resource-intensive. Incorporating machine learning techniques can enable more accurate and efficient prediction of concrete strength based on material composition and curing conditions. This study aims to address these gaps by evaluating the mechanical properties of alternative material-based concrete while also developing machine learning models to predict its compressive strength, thereby advancing sustainable and data-driven construction practices.

2. Materials, Methods and Methodology

2.1. Materials

Alternative materials such as fly ash, marble dust, laterite, and demolition debris were used as substitutes for conventional aggregates and cement in concrete mixtures designed for building structures. These materials were selected based on their availability, sustainability, and potential to enhance the mechanical properties of concrete. A visual representation of the materials used is shown in Figure 1. Ordinary Portland Cement (OPC) of grade 53, conforming to IS standards, was used as the primary cementitious component in the concrete mix. The cement had a specific gravity of 3.16 and a standard consistency of 31%. Its initial setting time was 60 minutes, while the final setting time was 320 minutes. Additionally, 10% Ground Granulated Blast Furnace Slag (GGBS) is incorporated as an additive. Fly ash a by-product of coal combustion, was utilized in varying proportions from 10% to 30%. Owing to its pozzolanic properties, fly ash helps improve the long-term strength and durability of concrete while also reducing environmental impact.

Table 1. *Properties of Materials*

Material	Property			
	Specific Gravity	Fineness modulus	Crushing value (%)	A I V (%)
Coarse aggregates	2.62	4.82	27	19
Demolition debris	2.45	4.75	28	21
Laterite	2.2	3.68	30	24
Fine aggregates	2.5	3.64	-	-
Fly ash	1.9	2.14	-	-
Marble dust	2.3	2.61	-	-

Specific gravity, which represents the density of a material relative to water, indicates that coarse aggregates (2.62) are denser than demolition debris (2.45) and laterite (2.2). This variation in density is significant, as denser materials, such as coarse aggregates, generally contribute to improved strength in concrete structures. The fineness modulus, which measures aggregate coarseness, is highest for coarse aggregates (4.82), indicating a rougher texture, while laterite (3.68) and marble dust (2.61) exhibit lower values, suggesting finer



Figure 1. *a) Natural aggregates b) River Sand c) Laterite d) Fly ash e) Marble Dust*

textures that can enhance the workability of the concrete mix. Furthermore, the crushing value, which reflects the strength of aggregates under load, is lower for coarse aggregates (27%) compared to laterite (30%), suggesting that laterite is relatively weaker. Similarly, the aggregate impact value (AIV), an indicator of toughness, follows a similar trend, with coarse aggregates exhibiting the lowest AIV (19%), whereas laterite (24%) and demolition debris (21%) demonstrate slightly lower resilience, potentially influencing the concrete's impact resistance. These material properties are crucial in selecting concrete components based on structural requirements such as strength and durability. For instance, aggregates with lower crushing values and AIV are preferable for high-strength and impact-resistant applications. Conversely, while laterite and demolition debris may slightly reduce strength and toughness due to their higher crushing values and AIV, they provide a sustainable alternative for environmentally conscious construction. Additionally, the lower specific gravity and fineness modulus of marble dust and fly ash contribute to enhanced workability while promoting sustainability. Therefore, the selection of materials should be optimized by balancing strength, durability, and environmental considerations, depending on the specific performance requirements of the concrete application.

2.2. Mix Proportion

The M30-grade concrete mix was designed with a proportion of 1:1.4:3.06 (cement: fine aggregate: coarse aggregate) and a water-cement ratio of 0.5. Before mixing, materials were weighed and assessed for quality to ensure compliance with concrete standards, as detailed in Table 1. Table 2 outlines the key properties of the concrete components. Marble dust, known for enhancing concrete performance, was incorporated at varying levels between 10% and 30%. Laterite, a naturally occurring material abundant in western Karnataka, India, was partially used to replace coarse aggregate. Composed of soil and rock, it is rich in iron and aluminium oxides and is commonly used in local construction for structural and cladding applications. The mix also included riverbed sand as fine aggregate and coarse aggregates from local quarries, both evaluated for specific gravity, fineness modulus, and water absorption. Clean, potable water was used, maintaining the specified water-cement ratio. The mix followed IS 456:2000(IS 456 2000) guidelines, prioritizing sustainable alternatives such as fly ash, marble dust, laterite, and demolition debris to improve both performance and environmental impact. Table 2 presents mix designs incorporating these alternative materials. Mixes M2 to M7 integrate marble dust and fly ash, aiming to enhance sustainability while maintaining workability, as their finer particle size improves mix fluidity. In contrast, mixes M8 to M14 replace coarse aggregates with laterite and demolition debris, offering eco-friendly alternatives to conventional aggregates. However, their lower specific gravity and higher crushing values suggest potential reductions in strength and toughness. Therefore, selecting these mixes requires balancing structural integrity with sustainability goals.

2.3. Sample preparation and Experimental Methods

Concrete specimens were prepared to evaluate the mechanical properties and durability properties of the mixes incorporating alternative materials. All specimens were cured in water for 7, 28, and 90 days

Table 2. *Concrete mix proportions*

Mix No.	Materials	C+G (kg)	FA (kg)	MD (kg)	F (kg)	CA (kg)	LA (kg)	DW (kg)
M1	Normal	438.5	619.2	0	0	1342.2	0	0
M2	10% of MD	438.5	557.3	61.9	0	1342.2	0	0
M3	20% of MD	438.5	495.4	123.8	0	1342.2	0	0
M4	30% of MD	438.5	433.4	185.7	0	1342.2	0	0
M5	10% of F	438.5	557.3	0	61.9	1342.2	0	0
M6	20% of F	438.5	495.4	0	123.8	1342.2	0	0
M7	30% of F	438.5	433.4	0	185.7	1342.2	0	0
M8	10% of LA	438.5	619.2	0	0	1208.0	134.2	0
M9	20% of LA	438.5	619.2	0	0	1073.7	268.4	0
M10	30% of LA	438.5	619.2	0	0	939.5	402.6	0
M11	10% of DW	438.5	619.2	0	0	1208.0	0	134.2
M12	20% of DW	438.5	619.2	0	0	1073.7	0	268.4
M13	30% of DW	438.5	619.2	0	0	939.5	0	402.6
M14	40% of DW	438.5	619.2	0	0	805.3	0	536.8
C+G = Cement+ GGBS, FA = Fine aggregate, MD = Marble Dust, F = Fly Ash, CA = Coarse aggregate, LA = Laterite, DW = Demolition waste								

to ensure proper hydration, following IS 516:1959 (IS 516 1959) guidelines. Additionally, samples were subjected to seawater curing to examine strength variations.

a) Slump Test

The slump test was conducted in this work to evaluate the workability and consistency of the various concrete mixes (M1 to M14) prepared with materials such as marble dust, fly ash, laterite, and demolition debris as partial replacements for conventional aggregates and cement.

b) Compression Strength

For the compressive strength test, the prepared concrete cubes were tested using a compression testing machine, as per IS 516:1959(IS 516 1959). The test was performed on cubes od size 150mm X 150mm X 150mm after 7, 28 and 90 days of curing to measure strength development over time. This allowed for the comparison of early-age and longer-term strength properties of the concrete mixes containing the alternative materials.

c) Flexural Strength

The flexural strength test was conducted on the cast beams of size 150mm × 150mm × 750mm to assess the flexural strength of the concrete under bending. This test was also conducted following the guidelines set by IS 516:1959(IS 516 1959). Flexural strength is critical for assessing the performance of the concrete mix under real-world conditions, where the structure would be subject to bending forces due to various loads.

d) Split Tensile Strength Test

The split tensile test is a vital method for determining the tensile strength of concrete cylinders, essential for evaluating performance under load. In this study, concrete cylinders of size 150mmØ x 300mm were made from various combinations of alternative materials fly ash, marble dust, Laterite and demolition debris are subjected to this test to assess their mechanical properties. The test applies a compressive load along the specimen's diameter, leading to failure along the applied load plane. Results from the split tensile test, conducted according to IS 516:1959(IS 516 1959) standards, provide insights into the tensile behaviour of these mixes and their suitability for structural applications.

e) Water Absorption

For the Water Absorption Test, the concrete specimens were evaluated to determine their porosity and permeability characteristics. The test was conducted as per ASTM C642, where oven-dried specimens were weighed before and after immersion in water for a specified duration. The percentage increase in weight was recorded to assess the water absorption capacity of the concrete. This test helps in understanding the durability of concrete mixes incorporating alternative materials by analysing their ability to resist moisture ingress.

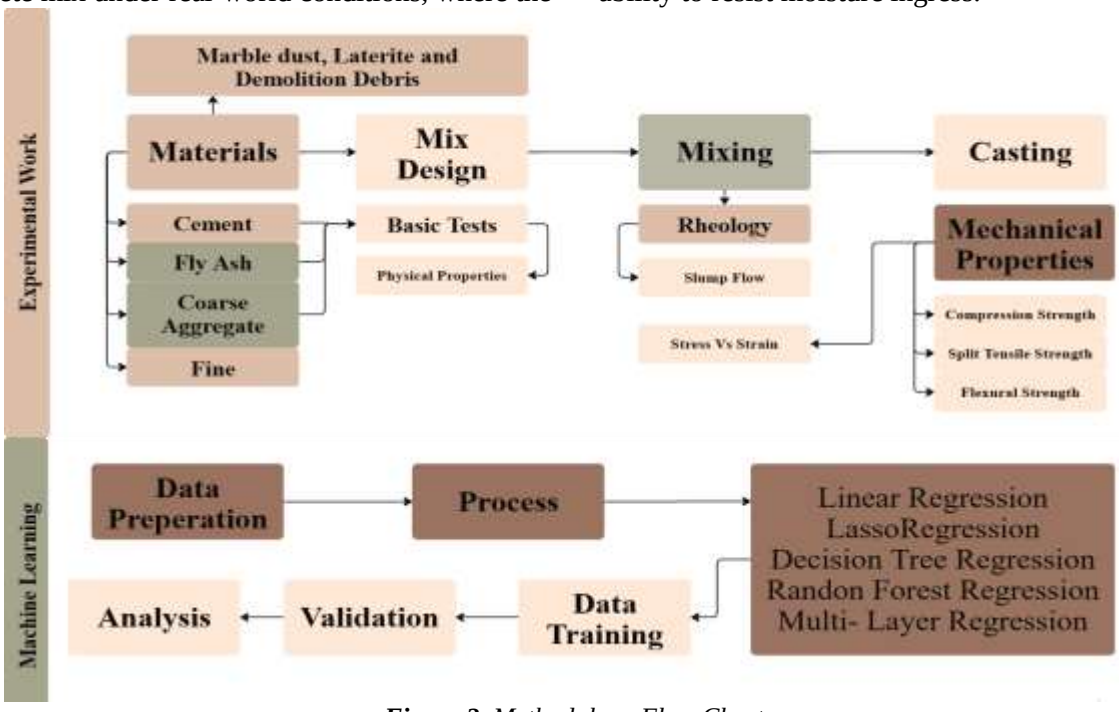


Figure 2. *Methodology Flow Chart*

f) Sorptivity

Sorptivity Test, the rate of capillary water absorption in concrete was measured following ASTM C1585. This test involved placing preconditioned specimens in contact with water and recording the weight gain at specified time intervals. The sorptivity coefficient was then calculated to evaluate the concrete's resistance to capillary suction, providing insights into its long-term durability and resistance to moisture penetration.

g) Rapid Chloride Permeability Test

Rapid Chloride Permeability Test (RCPT), the concrete specimens were tested as per ASTM C1202 to determine their resistance to chloride ion penetration. Cylindrical specimens were subjected to an electrical voltage of 60V for six hours, and the total charge passed (in coulombs) was recorded. This test helps assess the durability of concrete mixes containing alternative materials by measuring their susceptibility to chloride ingress, which is crucial for structures exposed to aggressive environments.

h) X-ray diffraction analysis

Concrete mix cubes were analysed by X-ray diffraction in JEOL X-ray diffractometer, using Cu-Kα radiation (1.542 Å) at 2θ of 2° /min. The morphology and chemical composition of oxides are examined and correlated with mechanical properties.

2.4. Methodology

The methodology consists of two sections Experimental Work and Machine Learning represented in Figure 2. In the experimental phase, various materials such as marble dust, laterite, and demolition debris, along with traditional components like cement, fly ash, coarse aggregate, and fine aggregate, are selected for the concrete mix. Basic tests to assess the physical properties of the materials followed by a proper mix design is formulated. The prepared mix then undergoes a thorough mixing process, where rheological tests such as slump flow analysis are conducted to evaluate its workability. After mixing, the concrete is cast into specimens, and mechanical properties including compressive strength, split tensile strength, and flexural strength are measured to determine the structural performance of the mix. In the machine learning phase, the data collected from experimental tests undergoes preparation and processing to ensure quality inputs for model training. Several regression models, including Linear Regression, Lasso Regression, Decision Tree Regression, Random Forest Regression, and Multi-Layer Regression, are employed to analyze and predict the concrete's mechanical properties. The trained models are validated to ensure their accuracy and reliability, followed by a detailed analysis of the results. This integrated approach of experimental testing and machine learning enables the prediction of concrete performance, optimizing mix designs and providing deeper insights into how alternative materials influence mechanical behaviour.

3. Machine Learning

3.1. Data Preparation

The dataset used for the machine learning models was compiled from 50 publications, consolidated into a single table, with the reference papers detailed in Table 4. It includes various factors such as compressive strength, cement, fine aggregate, coarse aggregate, water content, Ground Granulated Blast Furnace Slag (GGBS), marble dust, fly ash (F), laterite, and demolition waste. A final set of 590 samples was developed to analyse the compressive strength of concrete incorporating Ground Granulated Blast Furnace Slag (GGBS), marble dust, fly ash (F), laterite, and demolition waste.

3.2. Material Description

The primary component of concrete, cement, plays a crucial role in determining both early and long-term compressive strength. The water-to-cement ratio is a key factor in achieving the desired compressive strength, as an increase in water content generally results in a reduction in strength. The type of water used in the mix also influences strength development. The incorporation of Ground Granulated Blast Furnace Slag (GGBS), marble dust, fly ash (F), laterite, and demolition waste affects the overall performance of concrete. The application of fly ash is influenced by several factors, including the type of concrete, mix proportions, required workability, and curing conditions. Fly ash content can be gradually increased until an optimum dosage is reached, beyond which strength development declines. Similarly, marble dust, GGBS, and laterite contribute to strength enhancement up to a certain percentage, after which excessive replacement may lead to strength reduction. Since aggregate size is directly correlated with compressive strength, the inclusion of demolition waste as a coarse aggregate replacement also impacts strength development. The selection and proportioning of these materials require careful consideration to balance workability, strength, and sustainability.

3.3. Data Splitting

The dataset is initially partitioned into training and testing sets, with the training set typically being larger than the testing set. The model is first trained using the training dataset and then evaluated on the unseen testing dataset to assess its predictive performance. This approach ensures an objective evaluation of the model’s effectiveness on new data. After experimenting with various train-test split ratios, a 70% training split was identified as the most optimal and was consequently applied to all models in this study.

3.4. Performance Indices

Various machine learning models were developed to predict compressive strength. To assess and compare their predictive performance, four commonly used evaluation metrics were employed: Root Mean Square Error (RMSE), Mean Absolute Error (MAE), Mean Squared Error (MSE), and the Coefficient of Determination (R^2). Each of these metrics provides a unique insight into the model's accuracy and effectiveness, ensuring a comprehensive evaluation of its performance. Table 3 give the equation of different metrices.

3.4.1 Root Mean Square Error (RMSE)

RMSE measures the standard deviation of prediction errors, also known as residuals, by calculating the square root of the average squared differences between predicted and actual values. This metric is particularly useful as it assigns greater weight to larger errors, making it highly sensitive to outliers. A lower RMSE value indicates better model performance.

3.4.2 Mean Absolute Error (MAE)

MAE represents the average absolute difference between predicted and actual values, providing a direct interpretation of the average prediction error in the same units as the target variable. Unlike RMSE, MAE is less affected by outliers, making it a more robust measure of model accuracy.

3.4.3 Mean Squared Error (MSE)

MSE calculates the mean of the squared differences between predicted and actual values. Like RMSE, it penalizes larger errors more heavily, making it useful for model comparison. However, its interpretation is less intuitive due to the squared units.

3.4.4 Coefficient of Determination (R^2 Score)

R^2 quantifies the proportion of variance in the dependent variable that is explained by the independent variables. It ranges from 0 to 1, where 1 indicates a perfect fit, and 0 suggests that the model performs no better than using the mean of the dependent variable. This metric helps evaluate how well the model captures the variability in the data. Each of these metrics provides a unique perspective on model performance. RMSE and MSE are useful for comparing models and are particularly sensitive to large errors. MAE offers a straightforward measure of average error magnitude, while R^2 indicates the model's explanatory power relative to a baseline. Using these metrics collectively ensures a comprehensive assessment of each model's effectiveness in predicting concrete compressive strength.

3.5. Machine Learning Models

Table 3. *Equations of different performance indices*

Sl. No.	Performance Indices	Equation
1.	Root Mean square error	$RSME = \sqrt{(\sum_{-}(i = 1)\hat{}n \blacksquare (y - y\hat{}\,)\hat{}2/n)}$
2.	Mean absolute error	$MAE = \sum_{-}(i = 1)\hat{}n \blacksquare \lvert(y - y\hat{})/n\rvert$
3.	Median absolute error	$MedAE = median\{ \cup_{-}(i = 1)\hat{}n \blacksquare \llbracket \lvert y_i - y\hat{}_i \rvert \}\rrbracket$
4.	R^2 Score	$R\hat{}2 = 1 - (\sum_{-}(i = 1)\hat{}n \blacksquare (y - y\hat{}\,)\hat{}2\,)/(\sum_{-}(i = 1)\hat{}n \blacksquare (y - _y)\hat{}2\,)$

3.5.1.Linear regression

Linear Regression is a fundamental model used to predict continuous outcomes based on input features. It is trained on labelled data by adjusting its coefficients (weights and bias) to minimize the mean squared error between the predicted and actual values. This optimization is typically performed using gradient descent to determine the most suitable parameters. Equation is represented in table 4.

3.5.2.Lasso regression

Lasso Regression builds upon linear regression by introducing an L1 regularization term in the loss function, which encourages sparsity in the model coefficients. This feature selection capability helps reduce complexity and improve interpretability. While its training process is similar to that of linear regression, specialized optimization techniques such as coordinate descent are often employed to efficiently handle the L1 penalty. Equation is represented in table 4.

3.5.3.Random forest regression

Random Forest Regression enhances decision trees by constructing an ensemble of multiple trees. Each tree is trained on a bootstrap sample of the dataset, using a randomly selected subset of features at each split. The final prediction is obtained by averaging the outputs of all individual trees. This approach improves generalization and mitigates overfitting. Equation is represented in table 4.

3.5.4.Decision tree regression

Decision Tree Regression operates by recursively partitioning the input space based on feature values to minimize mean squared error within each subset. Unlike models that rely on gradient descent, decision trees use greedy algorithms to determine optimal split points, which serve as the model's parameters. This method enables straightforward interpretation but may require pruning to avoid overfitting. Equation is represented in table 4.

3.5.5.Multi-Layer Perceptron

Multi-Layer Perceptrons (MLPs) are a class of neural networks designed to model complex, non-linear relationships. They consist of multiple layers of interconnected neurons, each with unique weights and biases. MLPs are trained using backpropagation, a gradient-based optimization process that propagates errors backward through the network to update parameters. The objective is to minimize the mean squared error between the predicted and actual values, enhancing the model's predictive accuracy.

Table 4. *Equation of different models*

Sl. No	Model Name	Equation
1.	Linear regression	$\hat{y} = \theta_0 + \theta_1 x_1 + \theta_2 x_2 \dots\dots\dots + \theta_m x_m$ $J(\theta) = (\sum_(i=1)\hat{}n \blacksquare (y - y\hat{}\,)\hat{}2\,) /2n$
2.	Lasso regression	$J(\theta) = (\sum_(i = 1)\hat{}n \blacksquare (y - y\hat{}\,)\hat{}2\,)/2n + \alpha \sum_(i=1)\hat{}n \blacksquare \lvert\theta_i\rvert$
3.	Random forest regression	$J(\theta) = m_L \ \llbracket MSE \rrbracket_L + (m_r \ \llbracket MSE \rrbracket_R)/Mm$
4.	Decision tree regression	$J(\theta) = (\sum_(i = 1)\hat{}n \blacksquare (y - y\hat{}\,)\hat{}2\,)/2n + \alpha \sum_(i=1)\hat{}n \blacksquare \lvert\theta_i\rvert$

3.5.6.Exploratory Data analysis

The correlation heatmap presented in the Figure 3 provides a comprehensive analysis of the interrelationships between various attributes within the dataset. The correlation coefficients, ranging from -1 to 1, quantify the degree of linear association between the variables, with values closer to 1 indicating a strong positive correlation, values closer to -1 indicating a strong negative correlation, and values near 0 suggesting little to no correlation. Notably, the attributes C and G exhibit a perfect correlation (1.00), implying redundancy or a strong dependency between these variables. Similarly, the attributes CA and DW display a perfect negative correlation (-1.00), indicating an inverse relationship where an increase in one attribute corresponds to a proportional decrease in the other. Moderate positive correlations are observed between A and CS (0.63) and FA and LA (0.36), suggesting a potential interaction or complementary behavior among these variables. Conversely, FA exhibits negative correlations with both F (-0.62) and MB (-0.62), implying that as FA increases, these attributes tend to decrease. The presence of near-zero correlation values, particularly those expressed in scientific notation (2.8e-16), suggests numerical precision issues or attributes that may be nearly constant with minimal variation. These findings highlight key dependencies and interactions among the dataset variables, which are crucial for further statistical modelling and feature selection. The presence of redundant variables (C and G) may indicate the need for dimensionality reduction techniques, while highly correlated attributes (both positive and negative) could provide insights into underlying physical or chemical mechanisms governing the dataset.

4. Result and Discussions

4.1. Workability Properties

The Figure 4 presents the slump test results for different concrete mixes (M1 to M14), which provide an essential measure of workability and consistency. The slump values vary across the mixes, indicating how material composition influences the ease of handling and placement of concrete. Mixes incorporating fly ash (M5, M6, and M7) exhibit the highest slump values, ranging from 86 to 88 mm, reflecting excellent workability. This can be attributed to the fine particle size and smooth texture of fly ash, which improve the fluidity of the mix. In contrast, mixes containing marble dust (M1 to M4) demonstrate moderate workability, with slump values ranging from 80 to 85 mm. While marble dust enhances certain mechanical properties, its angular particle shape and lower packing density slightly reduce the mix's flowability. Meanwhile, mixes with laterite and demolition debris (M8 to M14) show the lowest slump values, between 62 and 77 mm, indicating reduced workability. The irregular particle shapes and increased water demand associated with these materials contribute to stiffer mixes. These results suggest that mixes with higher slump values are better suited for applications requiring easy placement and compaction, such as structural beams or columns. Conversely, lower slump mixes may need additional measures, such as the use of plasticizers or a higher water content, to improve workability. Overall, the slump test results provide critical insights into the practical applications of these concrete mixes, ensuring their suitability for specific construction scenarios.

4.2. Mechanical Properties

4.2.1.Compression Strength

Figure 5 presents the compressive strength results of various concrete mixes incorporating alternative materials such as fly ash, marble dust, laterite, and demolition debris, measured at curing ages of 7, 28,



Figure 3. *correlation between different attributes*

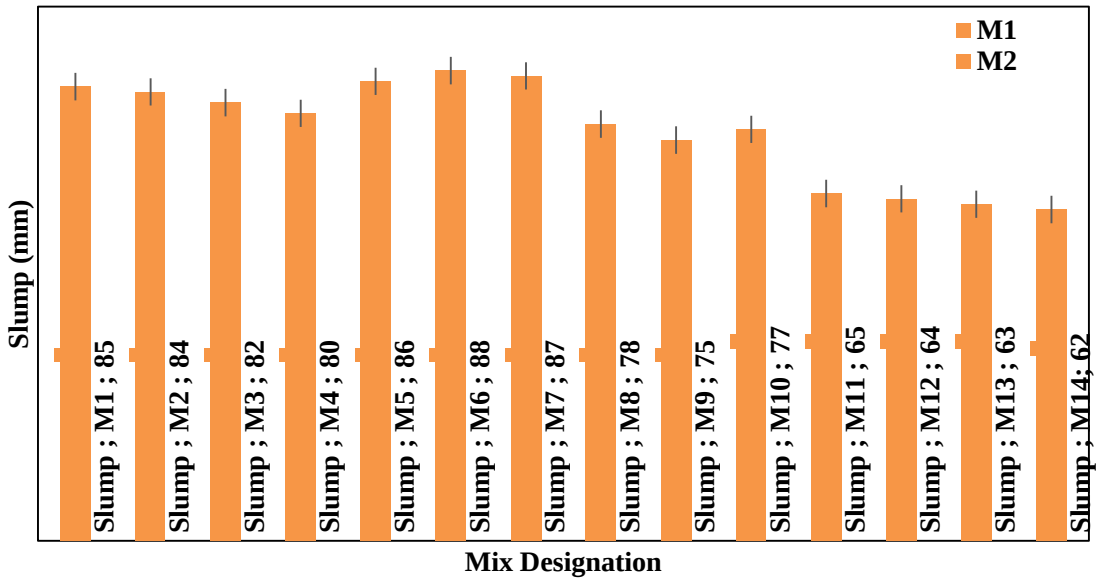


Figure 1. *Slump test for different concrete mixes*

and 90 days. These results provide insights into the performance characteristics of each mix in comparison to the control mix (M1), which serves as a benchmark for evaluating the viability of alternative materials. The conventional M1 mix achieved compressive strengths of 37.25 MPa at 7 days, 46.74 MPa at 28 days, and 51.31 MPa at 90 days, demonstrating consistent performance and establishing a reference for assessing the effects of material substitutions. The 10% fly ash mix (M5) exhibited compressive strengths of 35.61 MPa at 7 days, 45.09 MPa at 28 days, and 45.55 MPa at 90 days. While slightly lower than the control mix at early curing stages, the results highlight the pozzolanic activity of fly ash, which enhances long-term strength development. The delayed strength gain is attributed to the slow hydration process of fly ash, forming additional cementitious compounds over time. Despite the initial reduction, the comparable final strength suggests that fly ash is a viable and sustainable substitute for cement, contributing to improved concrete durability and reduced environmental impact.In contrast, the 30% marble dust mix (M4) exhibited a significant reduction in compressive strength, with values of 18.81 MPa at 7 days, 28.65 MPa at 28 days, and

28.94 MPa at 90 days. This decline is likely due to the poor binding properties of marble dust, which leads to increased porosity and reduced cohesion within the concrete matrix. The compromised structural integrity of M4 suggests that excessive marble dust replacement negatively impacts strength, making it less suitable for structural applications. These findings emphasize the need for careful proportioning to mitigate adverse effects on mechanical performance. Notably, the 10% laterite mix (M8) achieved a compressive strength of 48.95 MPa at 90 days, surpassing that of conventional concrete. Laterite, known for its rich iron and aluminium oxide content, enhances the binding properties of concrete when used in appropriate proportions. Its widespread availability further supports its use as a sustainable alternative to conventional aggregates, particularly in regions where it is naturally abundant. The improved performance of M8 underscores the potential of laterite as an effective material for enhancing concrete strength and durability while reducing dependence on natural resources.

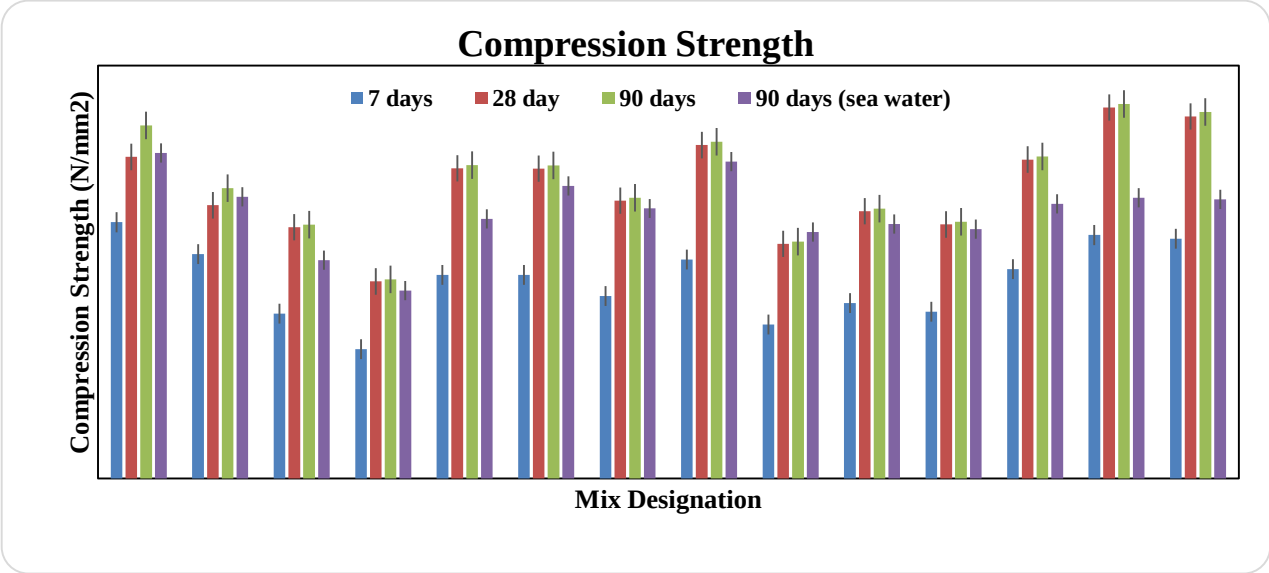


Figure 5. *Compression Strength of different mixes*

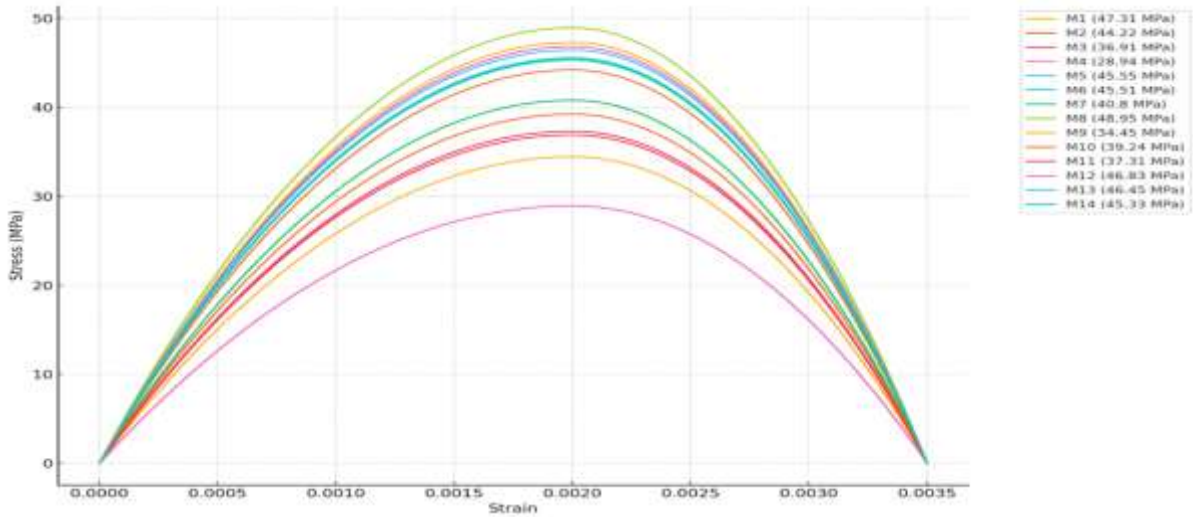


Figure 2. *Stress vs Strain for compression strength of different concrete mixes*

The stress-strain behaviour of the concrete mixes, as depicted in Figure 6, provides further insights into their mechanical response under compressive loading at 90 days. The x-axis represents strain, indicating the extent of deformation under stress, while the y-axis denotes stress, representing the applied force per unit area. Each curve reaches a distinct peak, corresponding to the maximum compressive strength, typically occurring at a strain of approximately 0.002—a characteristic of concrete's compressive properties. After reaching peak stress, the curves exhibit a gradual decline, signifying a controlled failure mechanism. This smooth post-peak response suggests a more ductile failure mode rather than a brittle fracture, which is advantageous for structural applications requiring

enhanced safety and energy absorption. Concrete mixes with higher compressive strengths, such as M8 (48.95 MPa), demonstrate superior load-bearing capacity and greater peak stress, whereas mixes with lower strengths, such as M4 (28.94 MPa), exhibit reduced mechanical performance, limiting their structural applicability. The post-peak slope of the curves also provides insights into the residual strength and ductility of each mix, aiding in the selection of materials based on specific construction requirements.

4.2.2.Flexural Strength

Figure 7 illustrates the flexural strength results of various concrete mixes incorporating fly ash, marble dust, and laterite, measured at 7, 28, and 90 days. Flexural strength is a critical parameter in assessing a concrete mix's resistance to bending or tensile forces, particularly in structural elements such as beams and slabs.

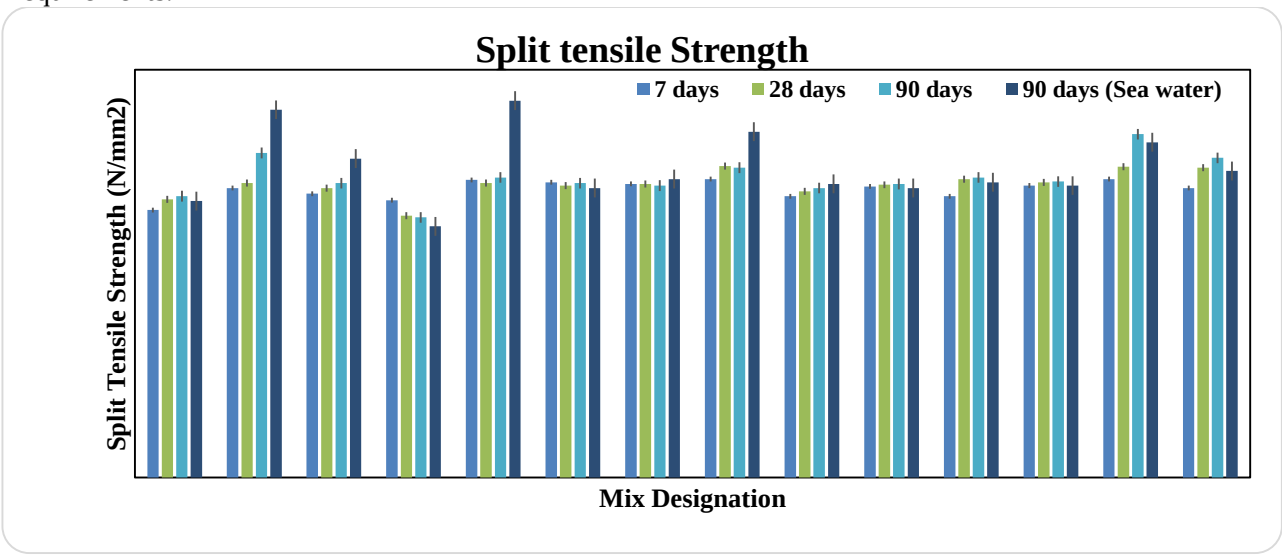


Figure 7. *Split tensile strength of different mix*

The control mix (M1) exhibited flexural strengths of 4.17 MPa at 7 days, 4.41 MPa at 28 days, and 4.58 MPa at 90 days, demonstrating reliable performance under loading conditions. These values serve as a benchmark for evaluating the effects of alternative materials on flexural behaviour. The 10% fly ash mix (M5) displayed strengths of 4.58 MPa at 7 days, 4.42 MPa at 28 days, and 4.58 MPa at 90 days, indicating a nearly consistent performance across curing periods. This suggests that fly ash can effectively replace a portion of cement without compromising flexural strength. The observed stability is attributed to the pozzolanic reaction of fly ash, which enhances bond strength and reduces porosity within the concrete matrix, contributing to improved durability. Incorporating marble dust produced varying results. The 10% marble dust mix (M2) demonstrated flexural strengths of 4.56 MPa at 7 days, 4.61 MPa at 28 days, and 4.82 MPa at 90 days, surpassing the control mix. However, higher marble dust content led to a decline in performance. The 30% marble dust mix (M4) recorded 4.61 MPa at 28 days and 4.52 MPa at 90 days, with a slightly lower value at 7 days. These findings suggest that while marble dust enhances early-stage strength, excessive replacement may reduce flexural capacity due to insufficient cementitious material and weakened bonding within the concrete matrix. The incorporation of laterite showed promising results. The 10% laterite mix (M8) achieved flexural strengths of 4.68 MPa at 7 days, 4.71 MPa at 28 days, and 4.82 MPa at 90 days, exceeding the control mix. This indicates that when used in appropriate proportions, laterite enhances flexural properties, making it a viable option for high load-bearing applications. However, the 30% laterite mix (M10) exhibited a slight reduction in flexural performance, with strengths of 4.44 MPa at 7 days, 4.55 MPa at 28 days, and 4.62 MPa at 90 days. This decline may be attributed to challenges in achieving adequate bonding and cohesion at higher laterite content.

Figure 8 illustrates the stress-strain behaviour of various concrete mixes (M1 to M14) under flexural loading, measured at 90 days. The graph provides valuable insights into the bending performance of each mix, highlighting key mechanical characteristics. Initially, all curves exhibit a linear relationship between stress and strain, representing the elastic phase, where the material deforms proportionally to the applied load. During this phase, the concrete retains its ability to return to its original shape upon load removal. Each curve reaches a peak point, corresponding to the maximum flexural strength of the mix, measured in megapascals (MPa).

This peak defines the highest stress the concrete can withstand before experiencing bending failure. The strain at peak stress is typically around 0.001, reflecting the material's flexibility under flexural forces. Beyond the peak, the curves gradually decline, marking the post-peak phase, where the material progressively loses its ability to bear stress. This gradual stress reduction signifies a ductile failure mode, in which the concrete retains some residual load-bearing capacity even after cracking.

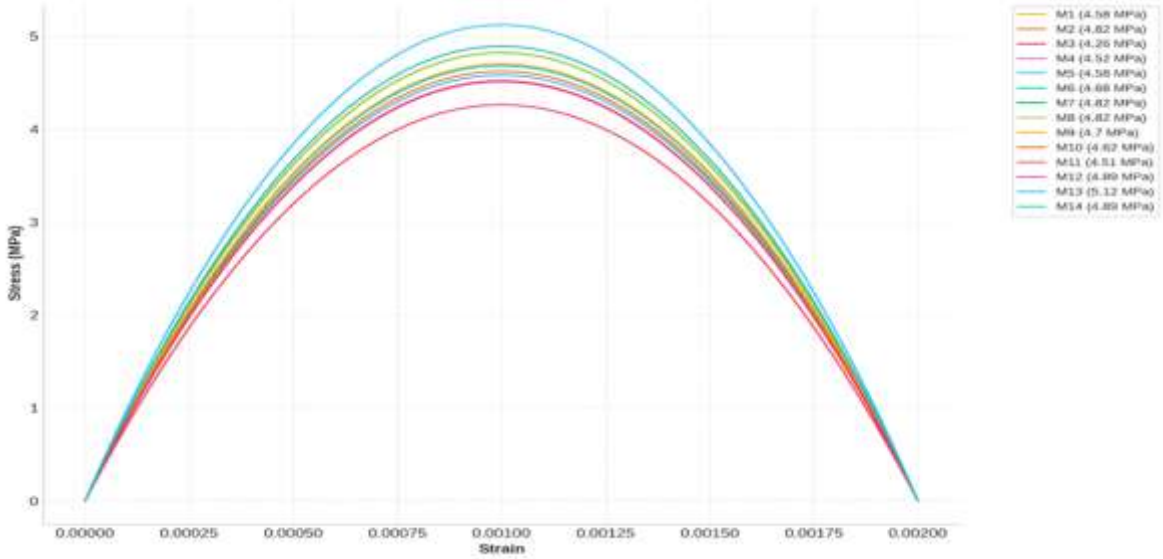


Figure 3. *Stress vs Strain for Flexural strength of different concrete mixes*

This behaviour contrasts with brittle failure, which would be characterized by a sudden and sharp drop in stress. Concrete mixes with higher flexural strengths, such as M13 with 5.12 MPa at 90 days, exhibit greater resistance to bending loads, represented by taller curves. Conversely, mixes with lower flexural capacities, such as M3 with 4.26 MPa, display shorter peaks, indicating reduced performance under bending stresses. The gradual decline after peak stress provides crucial insights into the ductility and residual strength of each mix, ensuring that the concrete can withstand real-world bending forces in structural applications like beams and slabs. This analysis is essential for selecting optimal concrete compositions that balance strength, durability, and flexibility, enhancing overall structural performance.

4.2.3.Split tensile Strength

Figure 9 presents the split tensile strength results for various concrete mixes incorporating fly ash, marble dust, laterite, and demolition debris at curing ages of 7, 28, and 90 days. The control mix (M1), composed of conventional materials, exhibited split tensile strengths of 3.28 MPa at 7 days, 3.41 MPa at 28 days, and 3.45 MPa at 90 days, serving as a benchmark for evaluating the performance of alternative materials. Among the modified mixes, the 10% fly ash mix (M5) demonstrated enhanced tensile properties, with strengths of 3.65 MPa at 7 days, 3.61 MPa at 28 days, and 3.68 MPa at 90 days. This improvement can be attributed to fly ash's pozzolanic reaction, which enhances the formation of cementitious compounds, improving bonding and structural integrity. Conversely, the 30% marble dust mix (M4) showed a significant reduction in split tensile strength, recording 3.40 MPa at 7 days, 3.21 MPa at 28 days, and 3.19 MPa at 90 days. The decline in strength is likely due to poor bonding and increased porosity caused by excessive marble dust, which weakens the concrete's resistance to tensile forces. The 10% laterite mix (M8) exhibited improved tensile performance, with strengths of 3.66 MPa at 7 days, 3.82 MPa at 28 days, and 3.80 MPa at 90 days. This suggests that laterite, when used in optimal proportions, enhances the tensile properties of concrete, making it a viable alternative where it is readily available. Additionally, the 30% demolition debris mix (M13) demonstrated notable tensile strength, achieving 3.66 MPa at 7 days, 3.81 MPa at 28 days, and 4.21 MPa at 90 days. The angular and rough texture of demolition debris likely contributed to better interlocking and bonding within the matrix, enhancing the mechanical properties of the concrete. Figure 10 illustrates the stress-strain behaviour of different concrete mixes (M1 to M14) based on their split tensile strength at 90 days. The initial phase of each curve shows a linear relationship between stress and strain, reflecting the elastic behaviour of the concrete, where deformation remains proportional to the applied stress. During this phase, the material can return to its original form upon load removal. Each curve reaches a peak stress point, representing the maximum tensile strength the mix can withstand before cracking.

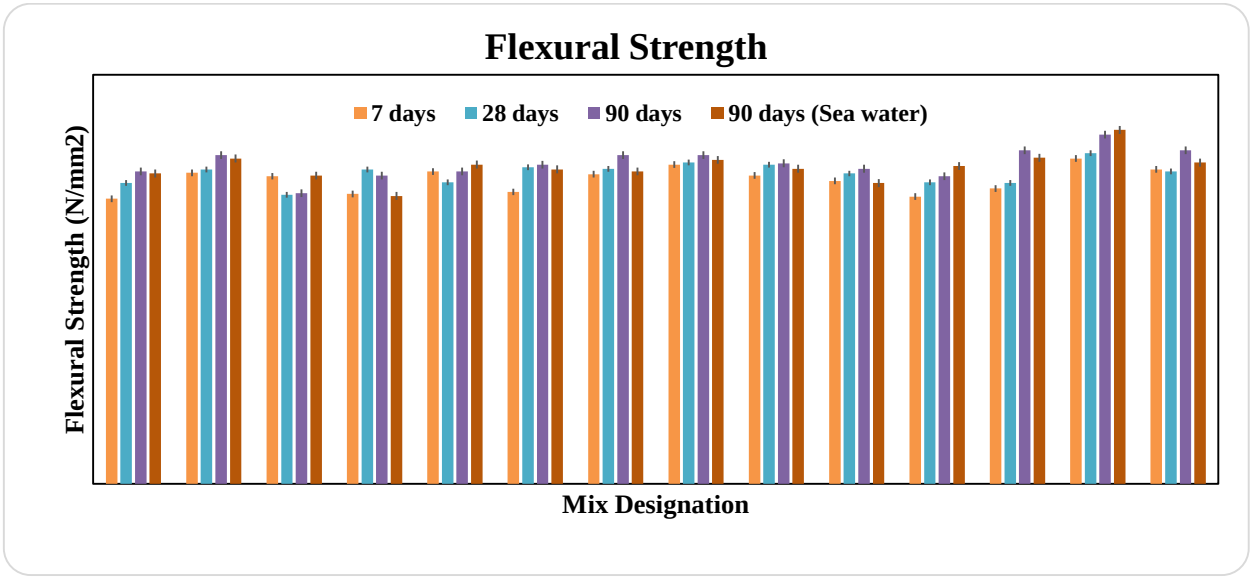


Figure 9. *Flexural Strength of different mix*

Among the mixes, M8 exhibited the highest peak tensile strength of 3.4 MPa, indicating superior resistance to tensile forces, whereas M4 recorded the lowest peak at 2.8 MPa, reflecting its reduced performance under tensile stress. Following the peak, the curves gradually decline, illustrating the post-peak phase, where the material progressively loses its ability to sustain tensile loads. This controlled failure behaviour highlights ductility, ensuring the concrete retains some residual strength rather than failing abruptly. Such characteristics are crucial in structural applications, particularly in columns, walls, and pipes, where tensile forces play a significant role.

4.3. Durability Properties

4.3.1. Water Absorption

Figure 11 illustrates the water absorption values of different concrete mix designations (M1 to M14), a crucial parameter influencing the durability and permeability of concrete. The values range approximately between 1.6% and 2.8%, showing significant variations among the mixes. M6 exhibits the highest water absorption (~2.8%), followed closely by M5 (~2.7%), indicating a more porous structure that may affect long-term durability. In contrast, M8 and M9 demonstrate the lowest absorption values (~1.6%-1.7%), suggesting a denser and less permeable concrete matrix. Mixes such as M1, M2, M4, M10, M11, and M12 fall within the moderate absorption range of 2.3%-2.6%, maintaining a balance between permeability and compactness.

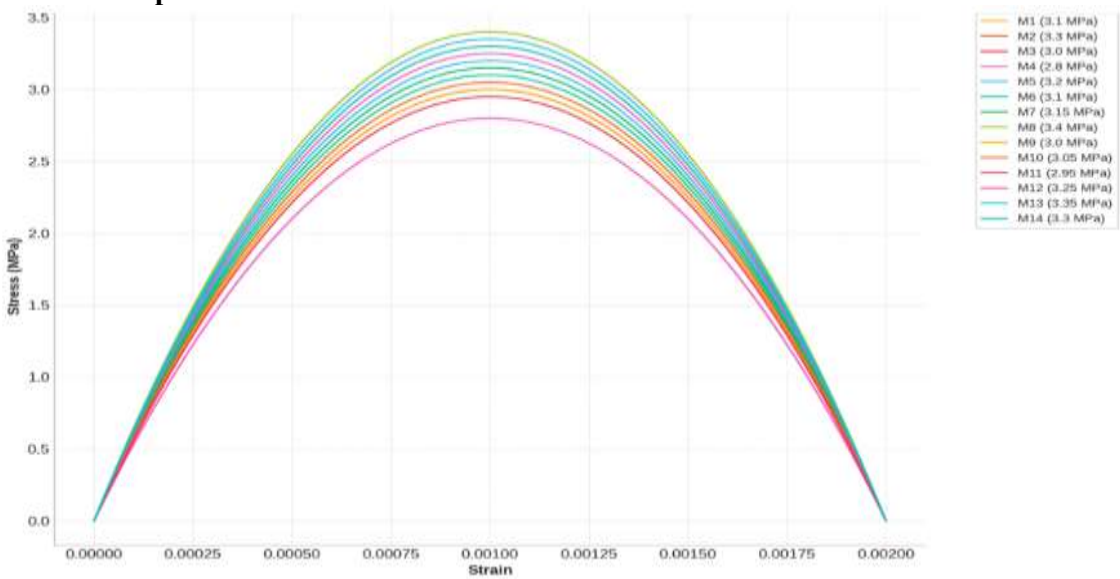


Figure 4. *Stress strain curves for Split tensile strength test*

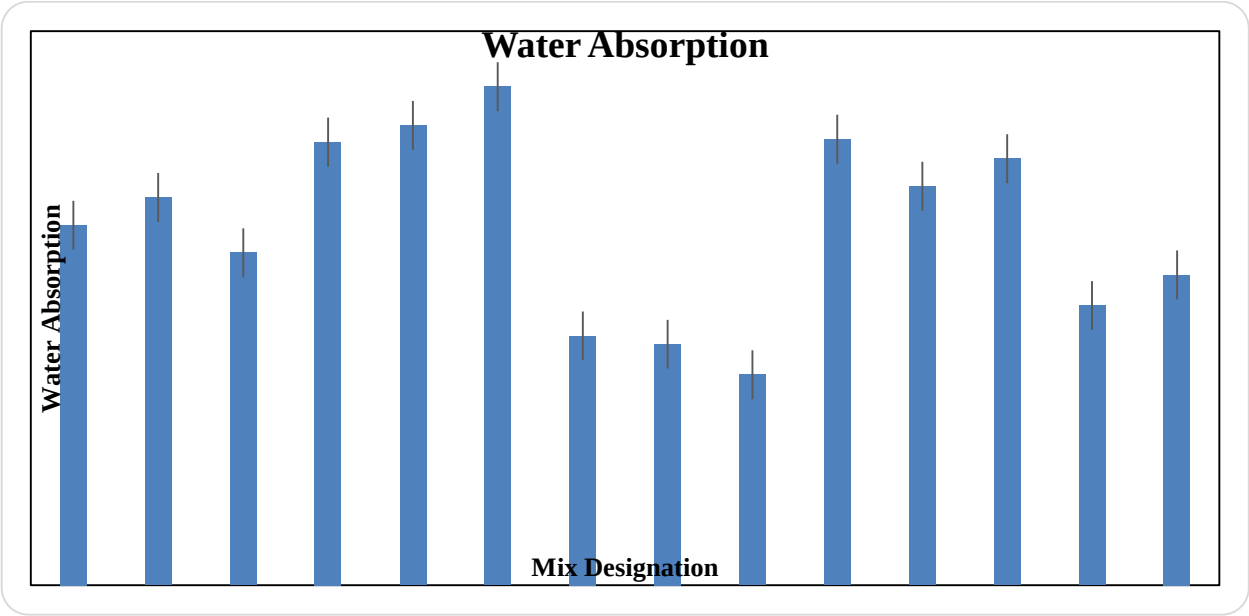


Figure 11. *Water absorption of different mix*

The error bars, representing standard deviation, confirm the reliability of the results, with small variations ensuring consistency in data collection.
The differences in water absorption can be attributed to material composition, particularly the use of fish scale powder, egg shell powder, recycled aggregate, or steel mill scale, which influence pore structure and water retention capacity. Higher water absorption suggests increased porosity, which could lead to moisture ingress, chloride penetration, and freeze-thaw damage, potentially reducing concrete durability. Conversely, lower absorption values indicate a denser mix with improved resistance to environmental exposure. These findings are critical in optimizing sustainable concrete mixtures, particularly in self-compacting concrete (SCC) applications, where achieving an optimal balance between workability, strength, and long-term durability is essential for enhanced structural performance.

4.3.2. Sorptivity

Figure 12 presents the sorptivity values for different concrete mix designations (M1 to M14), an essential parameter indicating the rate of capillary water absorption in concrete. The values range approximately between 1.3 and 1.9, highlighting variations in the permeability of the mixes. M8 and M9 exhibit the highest sorptivity (~1.9), suggesting a more porous microstructure that could lead to increased water ingress and reduced durability. In contrast, M10 and M11 show the lowest sorptivity (~1.3), indicating a denser mix with reduced capillary absorption, which enhances durability. Mixes M1, M2, M4, M5, and M6 fall within the moderate range of 1.5 to 1.7, maintaining a balance between permeability and compactness. The presence of error bars signifies standard deviation, ensuring the reliability and consistency of the results. The observed variations in sorptivity can be attributed to differences in material composition, particularly the incorporation of fish scale powder, egg shell powder, recycled aggregate, or steel mill scale, which influence the pore structure and water transport properties. Higher sorptivity values indicate increased capillary action, which could accelerate moisture ingress, chloride penetration, and potential deterioration, affecting long-term performance. Lower sorptivity, as seen in M10 and M11, suggests a more refined pore structure and enhanced resistance to water absorption, which is desirable for durable concrete. These findings are crucial for optimizing sustainable self-compacting concrete (SCC) mixtures, ensuring an ideal balance between workability, strength, and durability for enhanced structural performance.

4.3.3.Rapid Chloride Permeability Test

The bar chart illustrates the predicted Rapid Chloride Permeability Test (RCPT) results in Coulombs for various concrete mix designs (M1 to M14). RCPT measures the charge passed through a concrete specimen to assess its chloride permeability, with higher values indicating greater vulnerability to chloride penetration and corrosion. The results reveal significant variations among the mixes, with M9 exhibiting the highest RCPT value, exceeding 4000 Coulombs, suggesting poor chloride resistance. In contrast, mixes such as M3, M5, M6, M10, M11, and M12 demonstrate lower permeability, with RCPT values below 2500 Coulombs, indicating enhanced durability. The presence of error bars signifies the

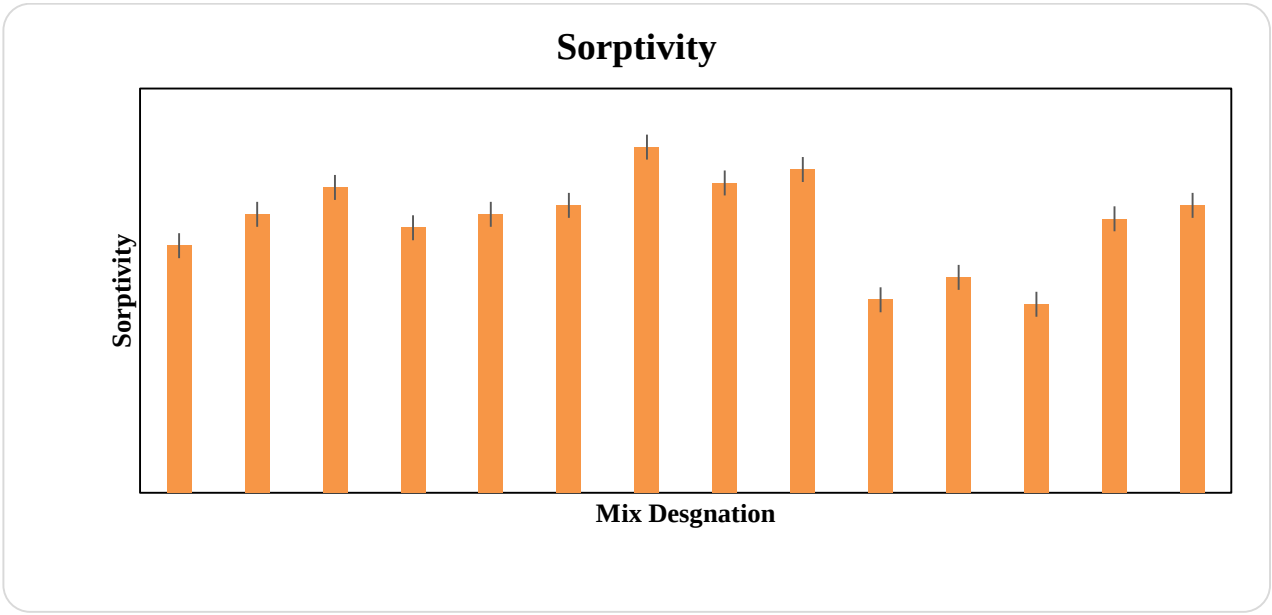


Figure 12. *Sorptivity results of different mix*

variability in predictions, possibly due to material inconsistencies or experimental uncertainty. These findings highlight the impact of mix composition on chloride resistance, where lower RCPT values are preferable for structures exposed to aggressive chloride environments, such as marine structures and bridges. Mixes with higher permeability, such as M9, may require modifications through supplementary cementitious materials like fly ash or silica fume to enhance durability. Understanding these permeability characteristics is crucial in optimizing concrete mixes for long-term structural performance.

4.4. Micro-Structure analysis

In this study, the XRD analysis of five different concrete mixes, M1 (control mix), M2 (marble dust mix), M5 (fly ash mix), M8 (laterite mix), and M11 (demolition debris mix), provides valuable insights into their mineralogical compositions and the impact of alternative materials on the mechanical properties of concrete, which is shown in figure 14.

4.4.1.M1 (Control Mix)

The control mix (M1), which consists of ordinary Portland cement (OPC), exhibits typical cementitious phases such as tricalcium silicate (C3S) and dicalcium silicate (C2S), with strong peaks observed at 29.3° and 32.5° for C3S and 33.1° for C2S, contributing to the compressive strength and early hydration of the concrete. The presence of calcium hydroxide (CH) is indicated by peaks at 18.0° and 34.1°, a by-product of cement hydration, confirming the conventional hydration process of OPC. These peaks indicate robust structural integrity and strength development in the control mix, with maximum intensity seen at 29.3° for C3S, reflecting its dominant contribution to early strength.

.

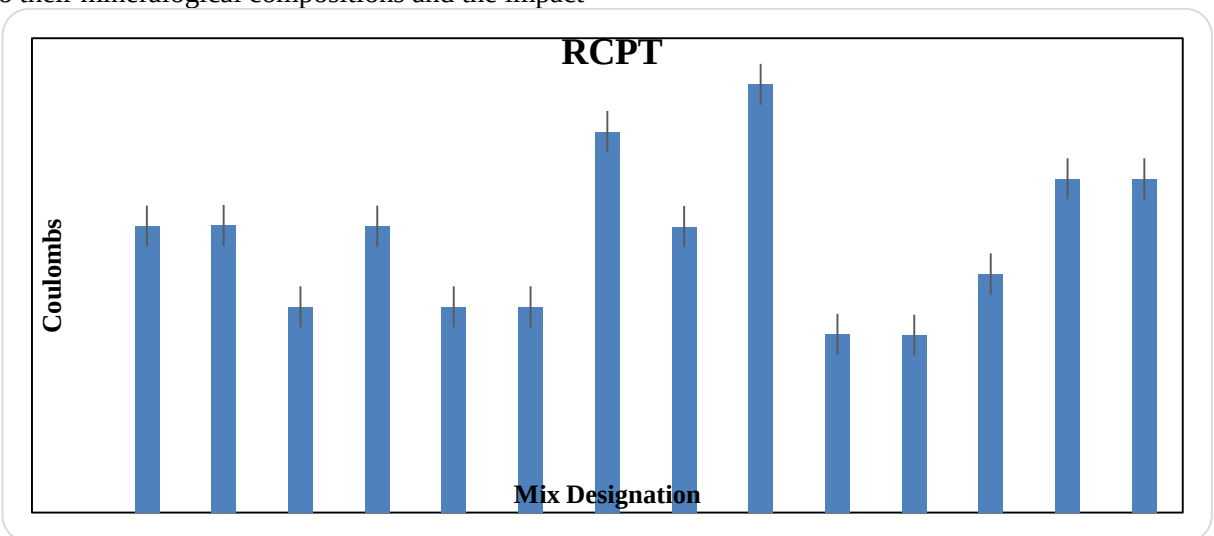


Figure 13. *RCPT Values of different mix*

4.4.2.M2-M4 (Marble Dust Mix)

The M2 mix, containing marble dust as a partial replacement for cement, shows distinct peaks for calcite ($CaCO_3$) at 23.1°, 29.4°, and 39.5°, corresponding to the high calcium carbonate content of marble dust. These peaks dominate the XRD pattern, especially the peak at 29.4°, which has the highest intensity. While C3S and C2S phases are still present, their relative intensities are lower than in M1, due to the reduced cement content. The introduction of marble dust leads to a high content of calcite, enhancing the concrete's compressive properties but potentially reducing its tensile strength, as indicated by the lower intensities of the cementitious phases

4.4.3.M5-M7 (Fly Ash Mix)

The M5 mix incorporates fly ash (10%), which is reflected in the XRD pattern by the presence of quartz (SiO_2), with strong peaks at 20.8° and 26.6°, and mullite ($3Al_2O_3 \cdot 2SiO_2$), with peaks at 16.4° and 40.8°. The presence of hematite (Fe_2O_3) is observed at 24.2° and 33.2°, indicating iron oxide content in the fly ash. While C3S and C2S peaks remain visible, their intensities are slightly reduced, indicating the partial replacement of cement. The reduction in calcium hydroxide (CH) peaks (at 18.0° and 34.1°) demonstrates that fly ash actively reacts with CH to form additional calcium silicate hydrate (C-S-H), contributing to long-term strength. The enhanced presence of quartz and mullite improves the mechanical strength and durability of the concrete.

4.4.4.M8-M10 (Laterite Mix)

In the M8 mix, which contains laterite as a partial replacement for aggregates, significant peaks for goethite (FeO(OH)) are observed at 21.1° and 36.5°, along with peaks for hematite (Fe_2O_3) at 24.2° and 33.2°, indicating the high iron oxide content of laterite. The presence of quartz (SiO_2) is also noted, with peaks at 26.6°, contributing to the mix's structural strength. The remaining cementitious phases, such as C3S and C2S, are still present, but their intensities are lower due to the partial replacement of cement. The iron oxides from laterite contribute to the compressive strength and durability of the concrete, making it suitable for applications requiring higher mechanical performance.

4.4.5.M11-M14 (Demolition Debris Mix)

The M11 mix, which incorporates demolition debris, shows dominant peaks for quartz (SiO_2) at 20.8° and 26.6°, and calcite ($CaCO_3$) at 29.4° and 39.5°, indicating the presence of recycled concrete or limestone materials. Additionally, a peak for feldspar ($KAlSi_3O_8$) at 31.0° reflects the inclusion of ceramic or brick debris. The cementitious phases, such as C3S and C2S, are present but show reduced intensities due to the partial replacement with demolition debris. The XRD pattern confirms that recycled materials can still contribute to the mechanical properties of the concrete, with quartz and calcite providing strength, while the presence of feldspar indicates some heterogeneity in the mix.

4.5. Machine Learning

Table 5 provides descriptive statistics for multiple variables, likely related to concrete mix design or construction materials. The cement content (C) has a mean of 386.5 kg/m³ with a low standard deviation of 19.26, indicating minimal variation. Similarly, gravel (G) remains fairly consistent with a mean of 42.95 mm and a narrow range of 40 to 45 mm. However, fine aggregate (F) exhibits high variability, with a mean of 26.56 kg/m³ but a large standard deviation of 56.07, suggesting some mixes do not contain fine aggregate at all. Fly ash (FA) shows a moderate variation, with values typically ranging between 433 and 619 kg/m³, while micro silica (MB) and lime (LA) have extreme variations, as many samples have zero content while others contain significant amounts. The coarse aggregate (CA) has a mean of 1246.34 kg/m³, showing moderate variation with values spanning from 805.3 to 1342.2 kg/m³, indicating different mix designs. Dry water content (DW) also has a large spread, ranging from 0 to 537 kg/m³, implying its presence varies significantly across samples.

In contrast, water content (W) remains fairly stable, with a mean of 206.23 kg/m³ and a low standard deviation of 14.66, suggesting a consistent water-to-cement ratio across samples. Admixture (A) values range from 7 to 90, but the median is 21, meaning most mixes contain similar amounts. Finally, compressive strength (CS) varies significantly, with a mean of 21.34 MPa and a broad range between 6.04 and 55.88 MPa, indicating diverse mix designs and performance outcomes. The presence of variables with zero values and high variability suggests that different mix compositions were tested, likely aiming to optimize performance under various conditions.

Table 6 presents the performance metrics of various regression models used for predicting RCPT values, including Root Mean Squared Error (RMSE), Mean Squared Error (MSE), Mean Absolute Error (MAE), and the coefficient of determination (R^2). Among the models, the Random Forest Regressor exhibits the best performance, achieving the lowest RMSE (1.05), MSE (1.27), and MAE (0.81), along with the highest R^2 value of 0.99, indicating its strong predictive accuracy and minimal error.

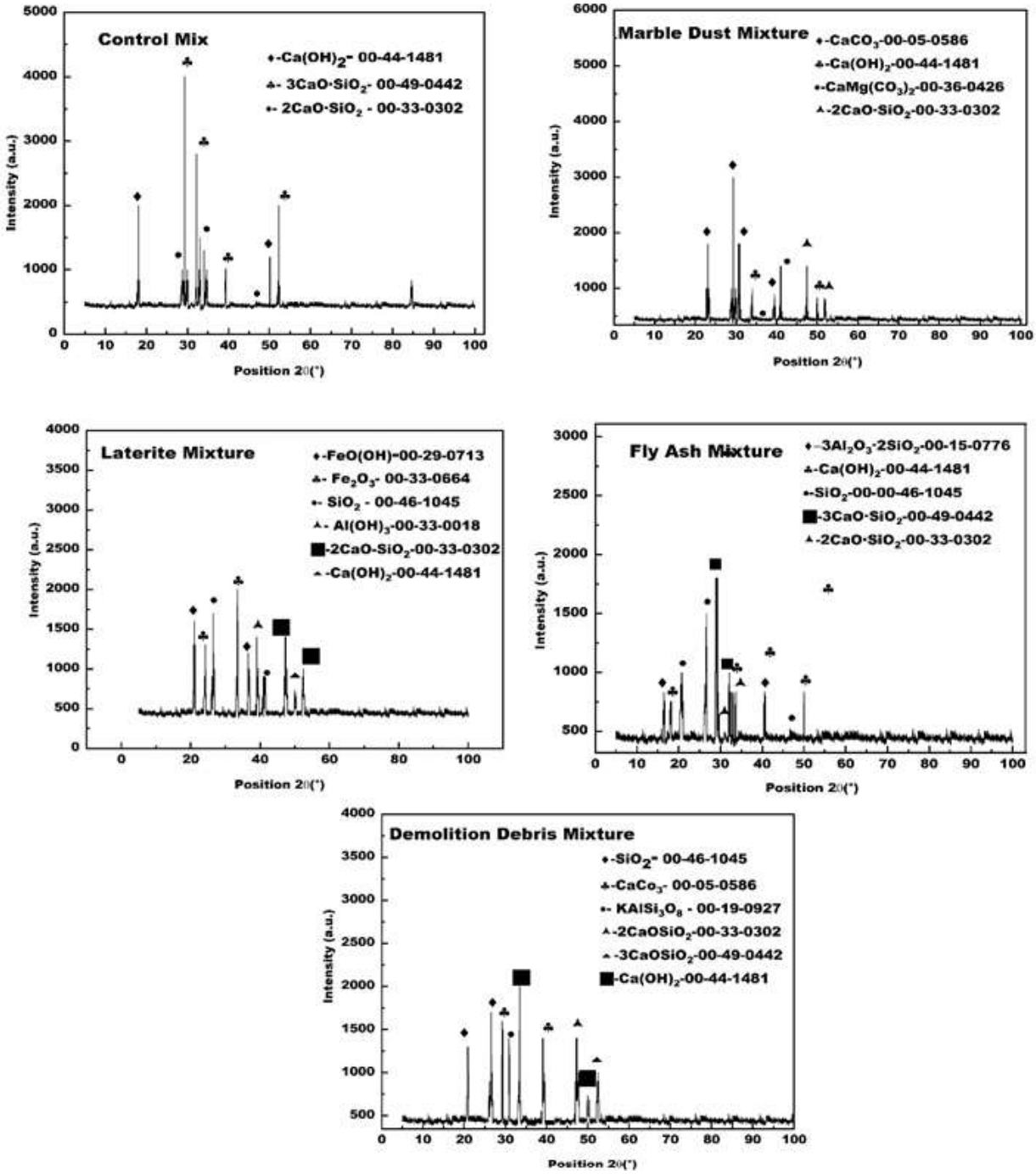


Figure 14. X-ray diffraction patterns of Concrete mixes

Table 5. *Statistics for multiple variables*

	Count	Mean	Std	Min	25%	50%	75%	Max
C	504	386.5	19.26	360	360	394.65	405	405
G		42.95	2.14	40	40	43.85	45	45
F		26.56	56.068	0	0	0	0	186
FA		565.87	69.82	433	495	619	619	619.20
MB		26.56	56.006	0	0	0	0	186
LA		57.50	121.39	0	0	0	0	403
CA		1246.34	171.6	805.3	1208	1342.2	1342.2	1342.2
DW		95.85	171.7	0	0	0	134	537
W		206.23	14.66	180	197.3	210.75	219.3	219.3
A		33	30.96	3	7	21	56	90
CS		21.34	12.15	6.04	23.78	32.89	40.54	55.88

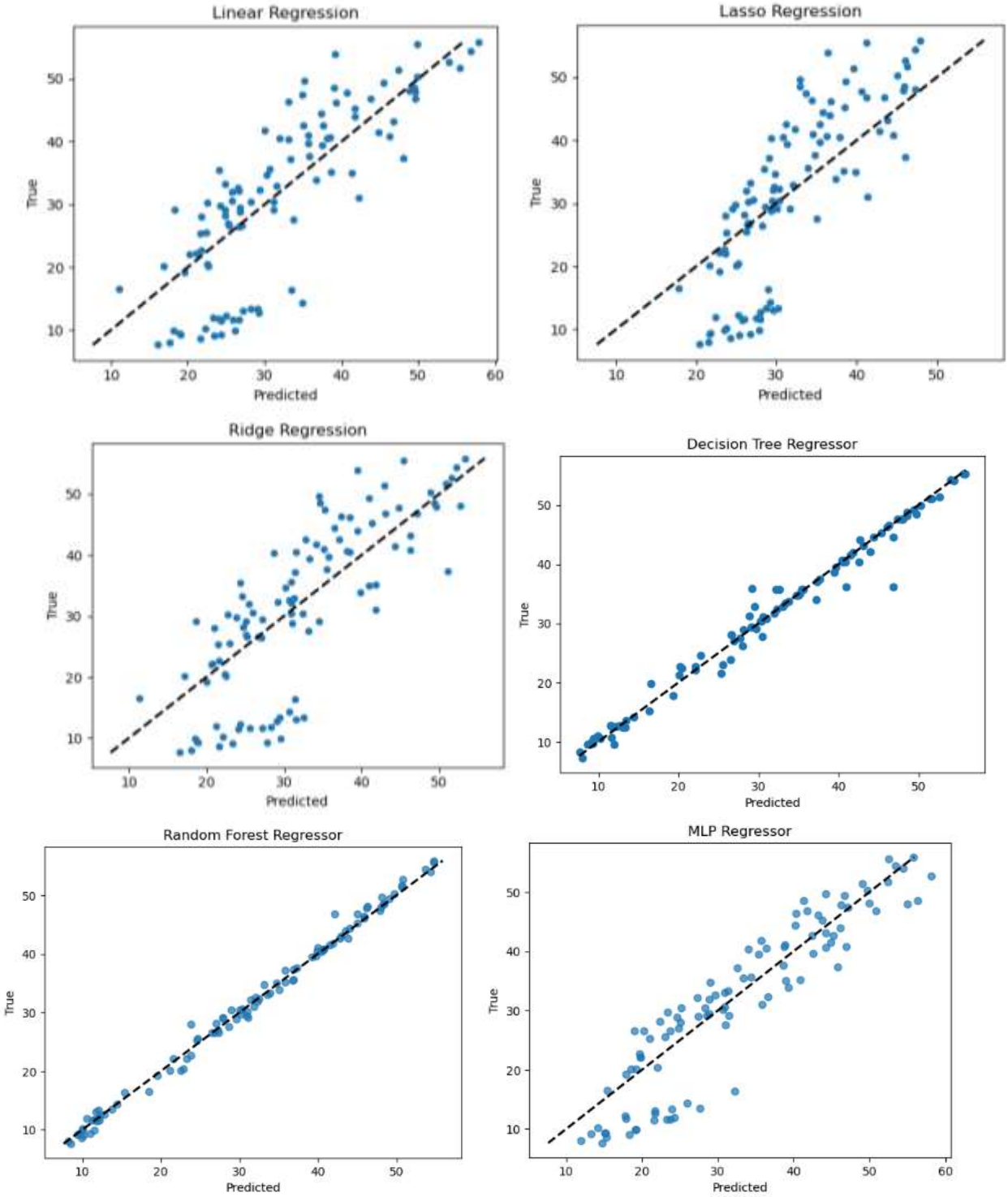


Figure 15. *Actual vs predicted of various regression models*

The Decision Tree Regressor also performs well with an RMSE of 3.50 and R^2 of 0.98, suggesting a good fit but with slightly higher errors compared to the Random Forest model. Traditional linear models such as Linear Regression, Lasso Regression, and Ridge Regression show moderate predictive ability, with RMSE values around 4.20 to 4.50 and R^2 values ranging from 0.57 to 0.65, implying a weaker correlation between the model predictions and actual values. The Multi-Layer Perceptron (MLP) model performs better than linear models, achieving an R^2 of 0.84, indicating improved predictive capability, but still falls short of the tree-based models. The significantly better performance of the Random Forest Regressor can be attributed to its ensemble learning approach, which reduces overfitting and enhances generalization. In contrast, linear models may struggle to capture complex nonlinear relationships in the dataset. These results suggest that tree-based models, especially Random Forest, are the

most suitable for predicting RCPT due to their superior accuracy and reliability.

Table 6. *Performance metrics of various regression models*

Models	RMSE	MSE	MAE	R^2
Linear Regression	4.20	17.62	3.90	0.65
Lasso Regression	4.50	20.25	4.10	0.57
Ridge Regression	4.30	18.49	4.00	0.61
Decision Tree Regressor	3.50	12.25	2.90	0.98
Random Forest Regressor	1.05	1.27	0.81	0.99
Multi-Layer Perceptron	4.00	16.0	3.80	0.84

5. Conclusion

This study concludes that incorporating alternative materials such as fly ash, marble dust, laterite, and demolition debris into concrete mixes offers promising potential for sustainable construction. These materials not only address the growing demand for environmentally friendly practices but also enhance or maintain the mechanical properties of concrete when used appropriately.

1. The results show that fly ash and laterite are particularly effective in improving compressive, flexural, and tensile strengths, making them excellent substitutes for traditional aggregates. Fly ash, when used in lower proportions (up to 10%), enhances strength without compromising the mix's performance, while laterite, especially at 10% replacement, outperforms conventional concrete mixes. These materials also bring the added benefits of cost-effectiveness and availability, particularly in regions with abundant local resources.
2. Demolition debris proved to be another valuable alternative, especially for boosting tensile strength due to its angularity and rough texture, which promote better bonding within the concrete matrix. However, while marble dust showed some potential at lower levels, excessive use negatively affected strength due to reduced cohesion and increased porosity, highlighting the need for careful material proportioning.
3. The study emphasizes the importance of balancing strength, sustainability, and workability when designing concrete mixes with alternative materials. It also demonstrates how these materials can reduce the reliance on natural resources, such as river sand and stone aggregates, without compromising the structural integrity of the concrete.
4. The application of machine learning in this study has proven to be a valuable tool for predicting and optimizing the mechanical properties of sustainable concrete. Various regression models, including Linear Regression, Lasso Regression, Decision Tree Regression, Random Forest Regression, and Multi-Layer Regression, were employed to analyse experimental data. Among these, the Random Forest Regression model exhibited the highest prediction accuracy with an R^2 value of 0.92, indicating its effectiveness in capturing complex relationships between mix proportions and concrete strength properties.

In summary, this research highlights the viability of using industrial by-products and recycled materials in concrete as a step toward sustainable construction. It also paves the way for future studies to explore the long-term durability of these mixes in real-world applications, ensuring their success in diverse environmental conditions.

Author Statements:

- **Ethical approval:** The conducted research is not related to either human or animal use.
- **Conflict of interest:** The authors declare that they have no known competing financial interests or personal relationships that could have appeared to influence the work reported in this paper
- **Acknowledgement:** The authors declare that they have nobody or no-company to acknowledge.
- **Author contributions:** The authors declare that they have equal right on this paper.
- **Funding information:** The authors declare that there is no funding to be acknowledged.
- **Data availability statement:** The data that support the findings of this study are available on request from the corresponding author. The data are not publicly available due to privacy or ethical restrictions.
- **Use of AI Tools:** The author(s) declare that no generative AI or AI-assisted technologies were used in the writing process of this manuscript.

References

[1] Ahmad, J., K. J. Kontoleon, A. Majdi, M. T. Naqash, A. F. Deifalla, N. Ben Kahla, H. F. Isleem, and S. M. A. Qaidi. 2022. "A Comprehensive Review on the Ground Granulated Blast Furnace Slag (GGBS) in Concrete Production." *Sustain.*, 14 (14). https://doi.org/10.3390/su14148783.

[2] Aliabdo, A. A., A. E. M. Abd Elmoaty, and E. M. Auda. 2014. "Re-use of waste marble dust in the production of cement and concrete." *Constr. Build. Mater.*, 50: 28-41. Elsevier Ltd.

https://doi.org/10.1016/j.conbuildmat.2013.09.005 .

[3] Aslani, A., C. Hachem-Vermette, and R. Zahedi. 2023. "Environmental impact assessment and potentials of material efficiency using by-products and waste materials." *Constr. Build. Mater.*, 378 (March): 131197. Elsevier Ltd. https://doi.org/10.1016/j.conbuildmat.2023.131197.

[4] Atta, I., and E. S. Bakhoum. 2024. "Environmental feasibility of recycling construction and demolition waste." *Int. J. Environ. Sci. Technol.*, 21 (3): 2675-2694. Springer Berlin Heidelberg. https://doi.org/10.1007/s13762-023-05036-y.

[5] Cheng, Y., H. Shen, and J. Zhang. 2023. "Understanding the effect of high-volume fly ash on micro-structure and mechanical properties of cemented coal gangue paste backfill." *Constr. Build. Mater.*, 378 (March): 131202. Elsevier Ltd. https://doi.org/10.1016/j.conbuildmat.2023.131202.

[6] Chun, Y., J. Kwon, J. Kim, H. Son, S. Heo, S. Cho, and H. Kim. 2023. "Experimental investigation of the strength of fire-damaged concrete depending on admixture contents." *Constr. Build. Mater.*, 378 (March): 131143. Elsevier Ltd. https://doi.org/10.1016/j.conbuildmat.2023.131143.

[7] Ettu, L. O., O. M. Ibearugbulem, J. C. Ezeh, and U. C. Anya. 2013. "The Suitability of Using Laterite as Sole Fine Aggregate in Structural Concrete." *Int. J. Sci. Eng. Res.*, 4 (5): 502-507. https://doi.org/10.13140/RG.2.2.36633.67688.

[8] Guo, Q., L. Chen, H. Zhao, J. Admilson, and W. Zhang. 2018. "The Effect of Mixing and Curing Sea Water on Concrete Strength at Different Ages." *MATEC Web Conf.*, 142: 1-6. https://doi.org/10.1051/matecconf/201714202004.

[9] Handayani, A. F., D. F. Muhammad, M. A. Hidayatullah, and N. L. Sari. 2023. "Pozzolanic properties of marble industrial waste and its used in concrete." *G-Tech J. Teknol. Terap.*, 7 (3): 1083-1090. https://doi.org/10.33379/gtech.v7i3.2765.

[10] Hussain, F., F. Rehman, R. A. Khushnood, S. Ali Khan, and A. Hamza. 2023. "Study of physical and mechanical behavior of artificial lightweight aggregate made of Pakistani clays." *Constr. Build. Mater.*, 378 (March): 131103. Elsevier Ltd. https://doi.org/10.1016/j.conbuildmat.2023.131103.

[11] IS 456. 2000. "Plain Concrete and Reinforced." *Bur. Indian Stand. Dehli*, 4: 1-114.

[12] IS 516. 1959. "Method of Tests for Strength of Concrete." *Bur. Indian Stand.*, 1-30.

[13] Joseph, H. S., T. Pachiappan, S. Avudaiappan, N. Maureira-Carsalade, Á. Roco-Videla, P. Guindos, and P. F. Parra. 2023. "A Comprehensive Review on Recycling of Construction Demolition Waste in Concrete." *Sustain.*, 15 (6). https://doi.org/10.3390/su15064932.

[14] El Khessaimi, Y., Y. El Hafiane, A. Smith, C. Peyratout, K. Tamine, S. Adly, and M. Barkatou. 2023. "Machine learning-based prediction of compressive strength for limestone calcined clay cements." *J. Build. Eng.*, 76 (March): 1-25. https://doi.org/10.1016/j.jobe.2023.107062.

[15] Kumar, G. S., M. S. Ujwal, H. A. Kumar, Y. H. Sudeep, and G. Venkatesha. 2025. "Evaluating the impact of spent coffee grounds on concrete's workability and mechanical properties using response surface methodology." *Innov. Infrastruct. Solut.*, 10 (2). Springer International Publishing. https://doi.org/10.1007/s41062-024-01843-5.

[16] Liu, B., S. Geng, J. Ye, X. Liu, W. Lin, S. Wu, and K. Qian. 2023a. "A preliminary study on waste marble powder-based alkali-activated binders." *Constr. Build. Mater.*, 378 (March): 131094. Elsevier Ltd. https://doi.org/10.1016/j.conbuildmat.2023.131094.

[17] Liu, C., B. Zhao, Y. Xue, Y. He, S. Ding, Y. Wen, and S. Lv. 2023b. "Synchronous method and mechanism of asphalt-aggregate separation and regeneration of reclaimed asphalt pavement." *Constr. Build. Mater.*, 378 (March): 131127. Elsevier Ltd. https://doi.org/10.1016/j.conbuildmat.2023.131127.

[18] Luo, Y., P. Guo, J. Gao, Y. Chen, D. Zhou, and J. Y. Hu. 2023. "Prediction and evaluation the moisture damage resistance of rejuvenated asphalt mixtures based on neural network." *Constr. Build. Mater.*, 378 (March): 131130. Elsevier Ltd. https://doi.org/10.1016/j.conbuildmat.2023.131130.

[19] Mali, A., S. Pastariya, S. Mehta, and A. Agnihotri. 2022. "Experimental Investigation on Partial Replacement of Laterite as Fine Aggregate in M20 Concrete." *Int. J. Res. Publ. Rev. J. homepage www.ijrpr.com*, 3 (06): 2304-2308.

[20] Mohamed, O. A., M. M. Hazem, A. Mohsen, and M. Ramadan. 2023. "Impact of microporous γ-Al2O3 on the thermal stability of pre-cast cementitious composite containing glass waste." *Constr. Build. Mater.*, 378 (March): 131186. Elsevier Ltd. https://doi.org/10.1016/j.conbuildmat.2023.131186.

[21] Olutoge, F. A., and A. G. Modupeola. 2014. "The effect of seawater on shrinkage properties of concrete." *Int. J. Res. Eng. Technol.*, 2 (March): 1-12.

[22] Singh, M., A. Srivastava, and D. Bhunia. 2019. "Long term strength and durability parameters of hardened concrete on partially replacing cement by dried waste marble powder slurry." *Constr. Build. Mater.*, 198: 553-569. Elsevier Ltd. https://doi.org/10.1016/j.conbuildmat.2018.12.005

[23] Singh, R. P., K. R. Vanapalli, V. R. S. Cheela, S. R. Peddireddy, H. B. Sharma, and B. Mohanty. 2023. "Fly ash, GGBS, and silica fume based geopolymer concrete with recycled aggregates: Properties and environmental impacts." *Constr. Build. Mater.*, 378 (March): 131168. Elsevier Ltd. https://doi.org/10.1016/j.conbuildmat.2023.131168.

[24] Ujwal, M. S., G. S. Kumar, R. Mahesh, and H. K. Ramaraju. 2025. "Modelling the mechanical properties of self compacting concrete with egg shell powder as supplementary cementitious material." *Multiscale Multidiscip. Model. Exp. Des.*, 8 (4). Springer International Publishing. https://doi.org/10.1007/s41939-025-00792-5.

[25] Ujwal, M. S., and G. Shiva Kumar. 2024. "A step towards sustainability to optimize the performance of

self-compacting concrete by incorporating fish scale powder: A response surface methodology approach." *Emergent Mater.*, (0123456789). Springer International Publishing. https://doi.org/10.1007/s42247-024-00786-y.

[26] Ulubeyli, G. C., and R. Artir. 2015. "Properties of Hardened Concrete Produced by Waste Marble Powder." *Procedia - Soc. Behav. Sci.*, 195: 2181-2190. Elsevier B.V. https://doi.org/10.1016/j.sbspro.2015.06.294.

[27] Wang, M., D. Chen, H. Wang, and W. Gao. 2024. "A review on fly ash high-value synthesis utilization and its prospect." *Green Energy Resour.*, 2 (1): 100062. The Authors. https://doi.org/10.1016/j.gerr.2024.100062.

[28] Zhao, H., S. Wang, R. Wang, L. Shen, and Q. Wang. 2023. "Utilization of raw coal gangue as coarse aggregates in pavement concrete." *Constr. Build. Mater.*, 378 (March): 131062. Elsevier Ltd. https://doi.org/10.1016/j.conbuildmat.2023.131062.

[29] Zia, A., P. Zhang, and I. Holly. 2023. "Effectiveness of hybrid discarded tire/Industrial steel fibers for improving the sustainability of concrete structures." *Constr. Build. Mater.*, 378 (March): 131226. Elsevier Ltd. https://doi.org/10.1016/j.conbuildmat.2023.131226.